191078. **Fine Structures of Refractivity in the Boundary Layer Revealed With a Polarimetric WSR-88D**

Valery Melnikov, Richard Doviak, Dusan Zrnic, and David Stensrud

University of Oklahoma, CIMMS and NOAA/OAR National Severe Storms Lab, Norman, OK

1. Introduction

Water vapor is the strongest contributor to the lower atmosphere's refractive index and, given the initial pressure, temperature and water vapor fields, changes in refractive index, and by proxy water vapor, near the ground can be monitored using radar measurements of changes in the phase path between the radar and stationary ground objects (Fabry et al. 1997; Fabry 2006). This phase path method provides spatial and temporal changes in the horizontal distribution of the refractivity field and water vapor in the lowest regions of the atmosphere to ranges of about 30 km. But this method does not reveal the height profile of either refractivity or water vapor.

Bragg backscatter from refractive index perturbations at scales half the centimetric and metric wavelengths of atmospheric radars, return sufficient energy to be useful in measuring wind and the refractive index structure parameter C_n^2, a parameter proportional to reflectivity η (e.g., Doviak and Zrnic 2006, chapter 11). As with the phase path measurements, water vapor perturbations in the CBL are the strongest contributor to C_n^2. But unlike phase path measurements, C_n^2 is strongly dependent on turbulent mixing in gradients of mean potential refractive index; Heinselman et al (2009) show if the reflectivity field obtained with the WSR-88D exhibits an elevated maximum, its height correlates well with the top of the CBL. If there are many biotic scatterers within the resolution volume, profilers cannot distinguish C_n^2 from reflectivity due to biota. However, the scanning polarimetric WSR-88D has the capability to distinguish echoes from atmospheric biota and Bragg scatterers and thus the potential to provide information on the temporal and spatial structure of C_n^2.

2. KOUN data in clear air

We collected radar data using dual-polarization S band WSR-88D situated at Norman, OK, i.e., KOUN radar. To enhance detectability of weak echoes and to reduce parameter estimate variance at low signal-to-noise ratios, the following data collection and signal processing procedures were implemented on KOUN: 1) increased the dwell time (i.e., 0.1s, yielding 128 samples at the pulse repetition frequency of 1280 Hz), 2) Collected data at smaller elevation increments (i.e., 0.25^o), 3)Doubled the range sampling rate, 4) Implemented a two-dimensional noise speckle remover to reduce the occurrence of false echoes, 5) Used covariance products to estimate differential reflectivity Z_{DR} and the correlation coefficient ρ_{hv}, 6) Collected data in vertical scans to elevations higher than 20^o to better resolve and interpret the fine details of reflectivity layers at close range, 7) Implemented ground clutter filtering at all elevation angles, and, 8) Coherently summed signals from the horizontal (H) and vertical (V) channels. Details of data collection and processing can be found in Melnikov et al. (2011).

By combining expressions for Z and reflectivity η of Bragg scatterers (e.g., Eqs. 4.31 and 11.104 in Doviak and Zrnic 2006), $\log_{10}$ [C_n^2 (m$^{-2/3}$)] can be expressed in terms of Z(dBZ) as, $\log_{10}$ [C_n^2 (m$^{-2/3}$)] = 0.1 Z(dBZ) – 11.6. The minimal C_n^2 is 3.5x10^{-15} m$^{-2/3}$ that corresponds to reflectivity of -28.5 dBZ. This level is more than two orders of magnitude below the mean C_n^2 value of 5x10^{-13} m$^{-2/3}$ measured with radar and an airborne refractometer in maritime boundary layer air over Oklahoma (Doviak and Berger 1980).

Using polarimetric radar, echoes from atmospheric biota can be distinguished from small water drop echoes because biota echoes typically have large positive Z_{DR} (dB) (Mueller and Larkin 1985; Wilson et al. 1994; Zrnic and Ryzhkov 1998; Lang et al. 2004). It was shown by Melnikov et al. (2011) that Bragg scatterers have Z_{DR} and ρ_{hv} properties similar to drizzle, these properties can then be used to distinguish Bragg and biota scatter under rain free conditions.

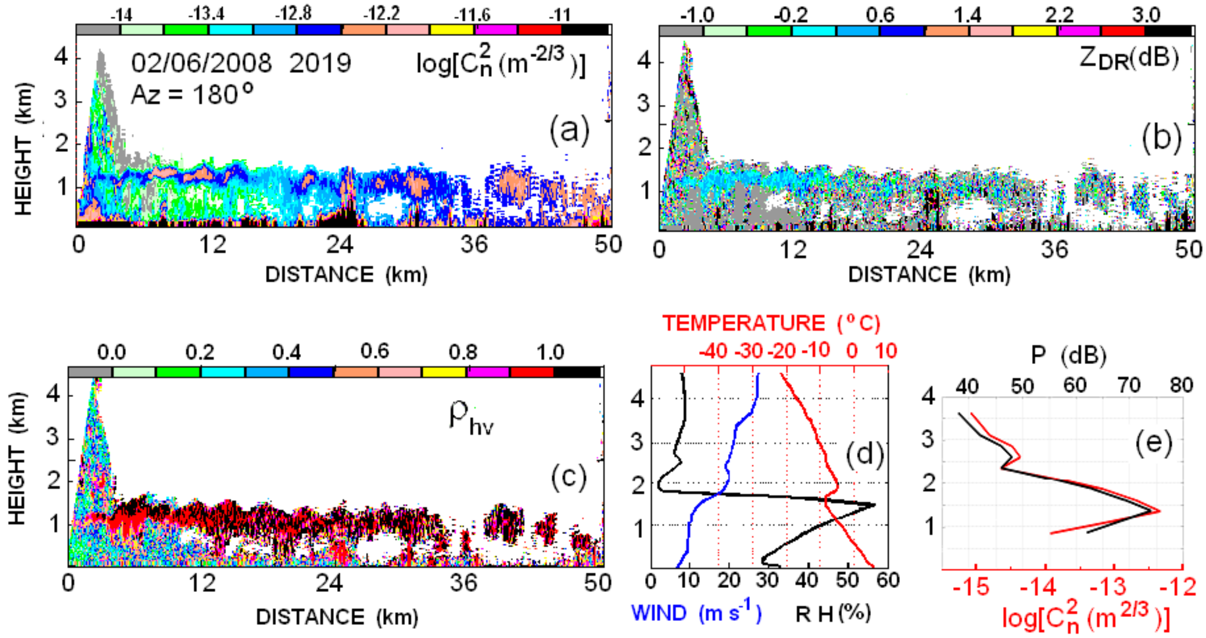

Fig. 1. Vertical cross-sections of (a) log(C_n^2), (b) Z_{DR}, and (c) ρ_{hv} fields. (d) Rawinsonde profiles of the temperature (red), wind velocity (blue), and relative humidity (black) above Norman, OK at 0Z February 27, 2008. (e) Echo power P (black) and estimated log(C_n^2) (red) from the NPN profiler at Vici, OK on 02/26/2008 at 2018 UT.

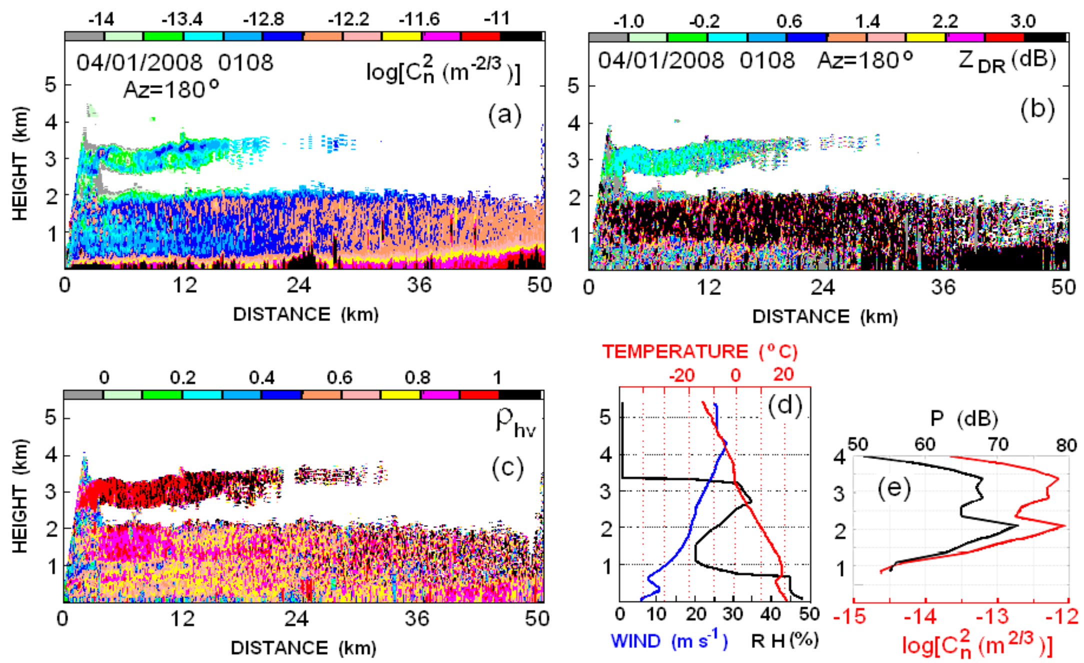

Fig. 2. Format is the same as in Fig. 1, but for data collected on April 1, 2008 at 0108 UT. Rawinsonde profiles (d) are for 0Z, and P and C_n^2 profiles (e) are from the NPN profiler at Purcell, OK.

In winter seasons, or for echo layer heights above the freezing level, where biota echoes are absent, our observations show mean ρ_{hv} is larger than 0.98, and comparisons of vertical profiles of C_n^2 from KOUN and those obtained from a 74.3 cm wavelength profiler from NOAA's Profiler Network (NPN) show good agreement in altitudes of maximums of C_n^2 from the profiler and KOUN and reasonable agreement in the magnitude of C_n^2 when conditions of horizontally homogeneity apply (e.g., Figs 1 c and g). In warm seasons, the boundary layer in Oklahoma is filled with biota. Sometimes layers of clear air echoes are observed above the biota (e.g., Fig. 2).

3. **Polarimetric properties of Bragg scatterers**

Although the polarimetric properties of Bragg scatterers have not been previously reported in the literature, the value of Z_{DR} is expected to be zero dB. This is so because the perturbations of the refractive index's scales that principally contribute to Bragg backscatter are 5-cm (i.e., half the radar wavelength, Doviak and Zrnic, 2006, Section 11.4). Such small scales are isotropic; therefore the mean and Z_{DR} should be 0 dB. As seen from Figs. 1 and 2, values of Z_{DR} are close to 0 dB as expected, and values of ρ_{hv} are close to unity in the layers of Bragg scatterers.

To obtain histograms of Z_{DR} and ρ_{hv} estimates, data with SNR > 5 dB have been used in all cases to eliminate large variations of estimates at lower SNR. Frequencies of occurrences of Z_{DR} and ρ_{hv} estimates are shown in Fig. 3. Based upon data from all cases examined, it is concluded that Bragg scatterers at 5-cm scales have $Z_{DR} \approx 0$ dB and $0.993 \leq \rho_{hv} \leq 1.0$. Thus, if sufficiently strong Bragg scatter can be confidently indentified with polarimetric radar, Bragg scatter can be used to check the system Z_{DR} bias of the WSR-88D. Echoes from Bragg scatterers should also give more reliable measurements of the radial velocity of wind without the bias as often is the case when biota are the scatterers in clear skies.

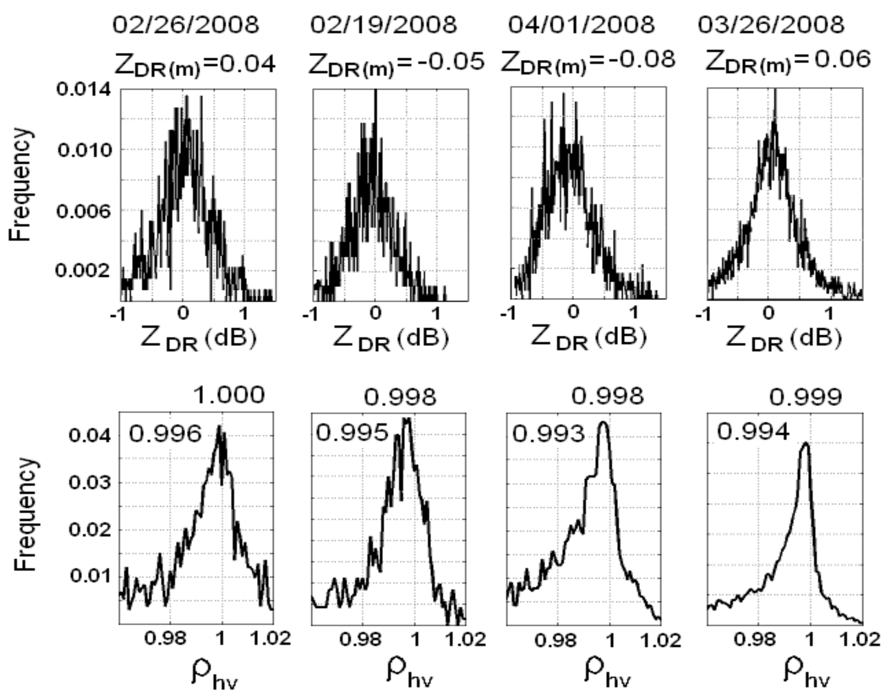

Fig. 3. Frequency of occurrences of Bragg scatter Z_{DR} and ρ_{hv} represented in columns for each observation. The last column is for drizzle with similar signal-to-noise ratios. The second top string shows heights above which the data were analyzed. $Z_{DR(m)}$ stands for the median value. Values of ρ_{hv} at the maxima of the histograms are presented at the tops of the ρ_{hv} panels, the values inside the panels stand for the median values of ρ_{hv}.

4. Mixed Bragg and biota scatter

In warm seasons in Oklahoma biota scatter frequently contaminates Bragg scatter. An example of a layer of Bragg scatterers imbedded into echo from biota is shown in Fig. 4. In panel (b), one can see a layer of reduced Z_{DR} at the height of about 2 km; ρ_{hv} have increased values in the layer in comparison with the surrounding areas. Panel (d) exhibits increased relative humidity in the layer. So presence of layers of reduced Z_{DR} and increased ρ_{hv} indicate Bragg scatter inside the echoes from biota.

Distinguishing biota and Bragg scatter might be accomplished by analyzing the H and V Doppler spectra. If the atmospheric fauna are migrating, their velocities can significantly differ from the wind and consequently wind measurements will be severely biased if the fauna are strong fliers (e.g., birds). If, by using spectral analysis, fauna echoes can be distinguished from Bragg scatter, more accurate wind measurement could be made with polarimetric Doppler radar. Spectra or portions of the spectra associated with backscatter from biota should exhibit large differences in spectral power densities at horizontal and vertical polarizations whereas spectra or portions of the spectra associated with Bragg scatterers should have very small or negligible spectral power differences. More discussions on the Doppler spectra can be found in Melnikov et al. (2011).

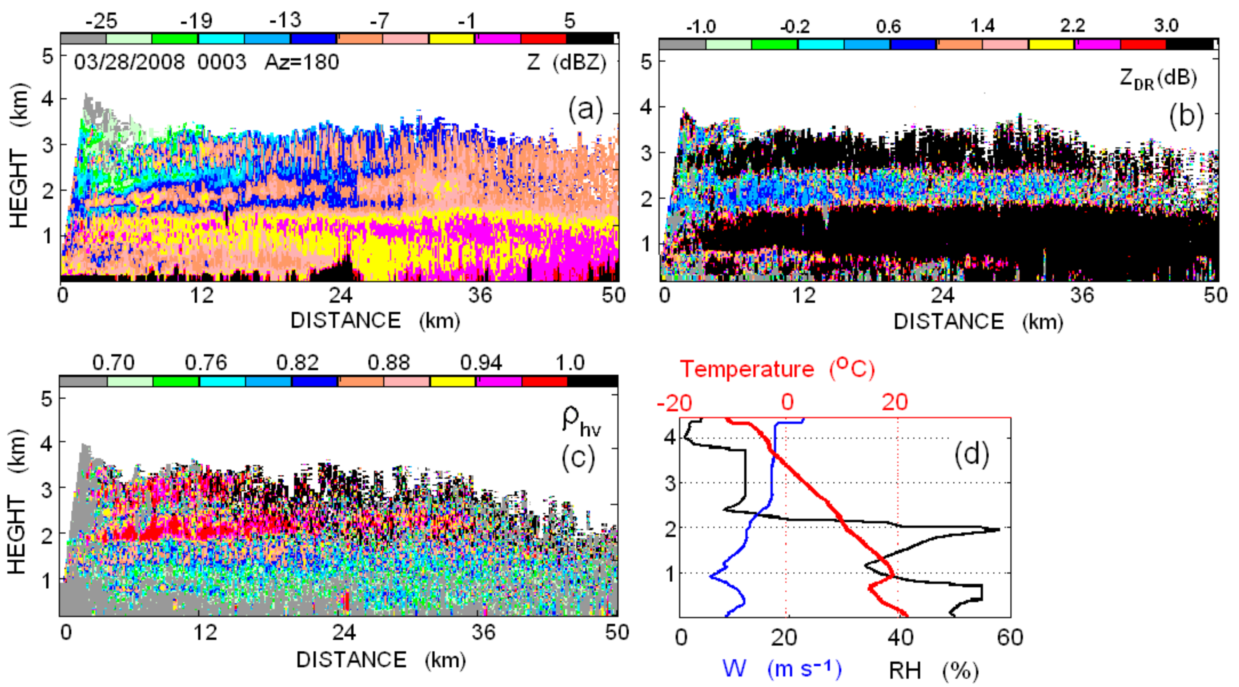

Fig.4. (a-c): Polarimetric fields on 28 March, 2008 at 0003Z and (d) rawinsonde profiles at 0000Z at Norman, OK.

5. Conclusions

- Observations with a dual polarization WSR-88D (KOUN) show the capability to measure C_n^2 as low as 3.5×10^{-15} $m^{-2/3}$ at a range of 10 km; this is about two orders of magnitude below the mean C_n^2 of 5×10^{-13} $m^{-2/3}$ measured with an airborne refractometer in maritime boundary layer air over Oklahoma (Doviak and Berger 1980). Observations with KOUN show significant advantage of having a scanning capability to map the horizontal extent and structure of C_n^2.

- In cases where "clear air" returns to KOUN are thought not to have been contaminated with airborne biota clutter, a good correspondence was found between the properties of echo layers observed with KOUN and with longer wavelength wind profilers. Thus the NPN profiler and WSR-88D networks have the potential to provide, by working in a coordinated approach, more reliable meteorological data.

- Medium differential reflectivities of Bragg scatterers, using enhanced data collection and processing procedures on KOUN, lie in the interval -0.08 to 0.06 dB . Thus it is concluded Bragg scatter at 10-cm wavelengths has $Z_{DR} \approx 0$ dB. The distributions of the measured Bragg scatter correlation coefficients ρ_{hv} have peaks between 0.998 and 1.0 with a median value of 0.995.

- Layers of Bragg scatterers have also been observed within echoes of biota. In some such cases slightly positive Z_{DR} (0.2 – 0.3 dB) and decreased ρ_{hv} (as low as 0.977 for the median value) are attributed to the presence of biota. In one case a layer of Bragg scatter was present at the top of the CBL, with biota both below and above. But polarimetric spectral analysis has the potential to better distinguish the two types of scatterers, even when both are present within the radar's resolution volume.

- Results suggest that one potential meteorological application of Bragg scatter mapping is monitoring the temporal and spatial changes in the depth of the CBL.

References

Doviak, R.J, and M.J. Berger, 1980: Turbulence and waves in the optically clear planetary boundary layer resolved by dual Doppler radars. *Radio Sci*., **15**, 297-317.

Doviak, R. J. and D. S. Zrnic, 2006: *Doppler radar and weather observations*, 2nd ed., Dover Publications, 562 pp.

Fabry, F., C. Frush, I. Zawadzki, and A. Kilambi, 1997: On the extraction of near-surface index of refraction using radar phase measurements from ground targets. *J. Atmos. Oceanic Technol.,* **14,** 978–987.

Fabry, F., 2006: The spatial structure of moisture near the surface: Project-long characterization. *Mon. Wea. Rev.,* **134,** 79–91.

Heinselman, P.L., D.J. Stensrud, R.M. Hluchan, P.L. Spencer, P.C. Burke, and K.L. Elmore, 2009: Radar reflectivity–based estimates of mixed layer depth. *J.Atmos. Oceanic Technol.*, **26**, 229–239.

Lang, T.J., S.A. Rutledge, and J.L. Smith, 2004: Observations of quasi-symmetric echo patterns in clear air with the CSU-CHILL polarimetric radar. *J. Atmos. Oceanic Technol.,* **21**, 1182-1189.

Melnikov, V.M., R. J. Doviak, D. S. Zrnić, and D. J. Stensrud, 2011: Mapping Bragg scatter with a polarimetric WSR-88D. *J. Atmos. Oceanic Technol*., Early release. doi: 10.1175/JTECH-D-10-05048.1.

Mueller, E.G., and R.P. Larkin, 1985: Insects observed using dual-polarization radar, *J. Atmos. Oceanic Technol*., **2**, 49-54.

Wilson, J.W., T.M. Weckwerth, J. Vivekanandan, R.M. Wakimoto, and R.W. Russel, 1994: Boundary layer clear-air radar echoes: Origin of echoes and accuracy of deriving winds. *J. Atmos. Oceanic Technol*., **11**, 1184-1206.